Supplementary Materials for

Intranasal administration of a single dose of a candidate live attenuated vaccine derived from an NSP16-deficient SARS-CoV-2 confers sterilizing immunity in animals

Zi-Wei Ye[1†], Chon Phin Ong[2†], Kaiming Tang[1†], Yilan Fan[1†], Cuiting Luo[1], Runhong Zhou[1], Peng Luo[1], Yun Cheng[2], Victor Sebastien Gray[2], Pui Wang[1,3], Hin Chu[1,3], Jasper Fuk-Woo Chan[1,3], Kelvin Kai-Wang To[1,3], Honglin Chen[1,3], Zhiwei Chen[1,3], Kwok-Yung Yuen[1,3], Guang Sheng Ling[2]*, Shuofeng Yuan[1,3]*, Dong-Yan Jin[2]*

The PDF file includes:

Figs. S1 to S7

Table S1

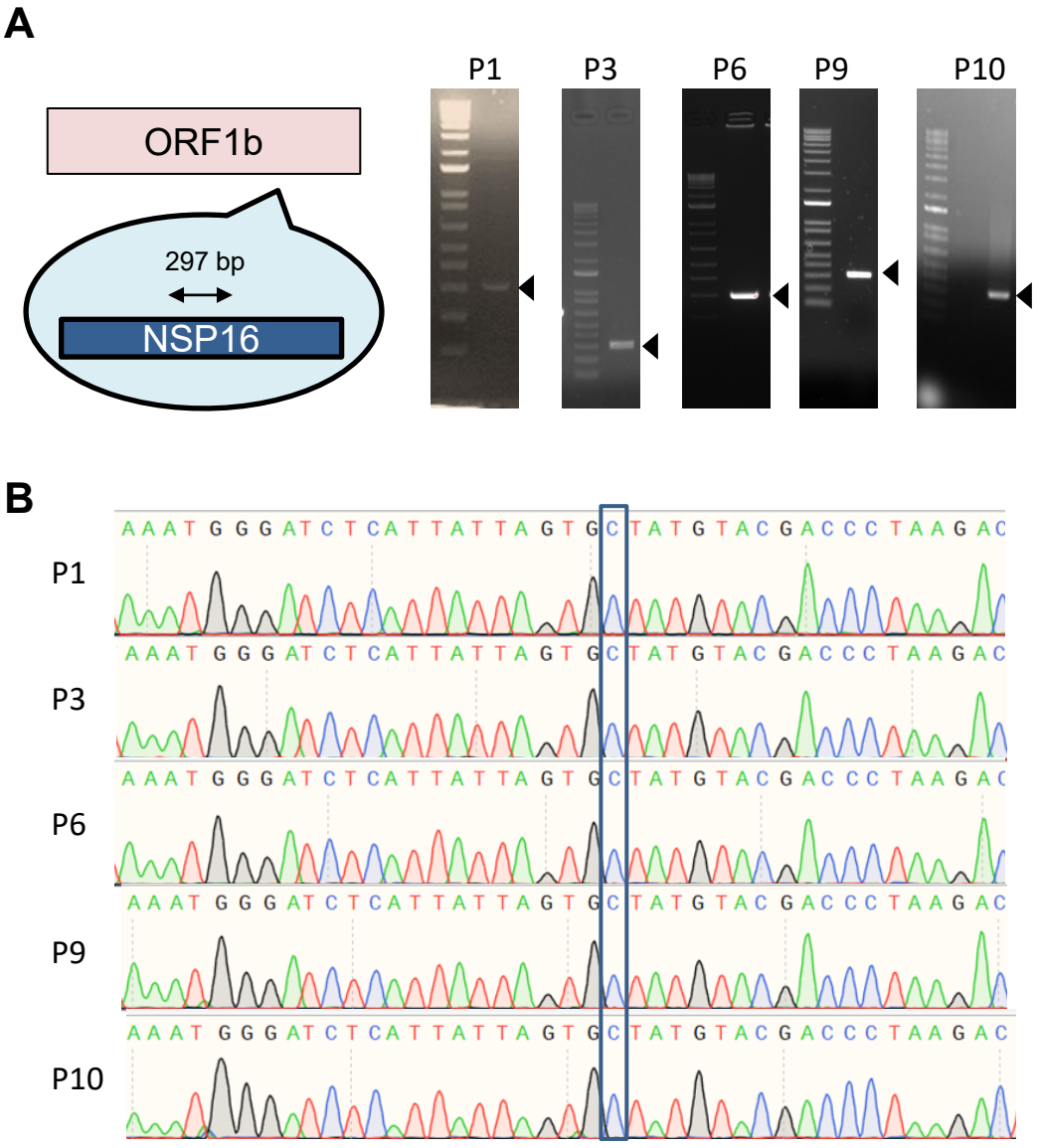

Fig. S1. Genetic stability of SARS-CoV-2 d16. A Detection of d16 gene during viral passage in VeroE6 cells. RNAs were extracted from the d16-infected cells of P0 to P10 passages. RT-PCR was performed with a primer pair flanking the d16 mutation. The 297-bp PCR products were resolved by agarose gel electrophoresis (arrowhead). The passage numbers were denoted at the top of each lane. **B** Sanger sequencing.

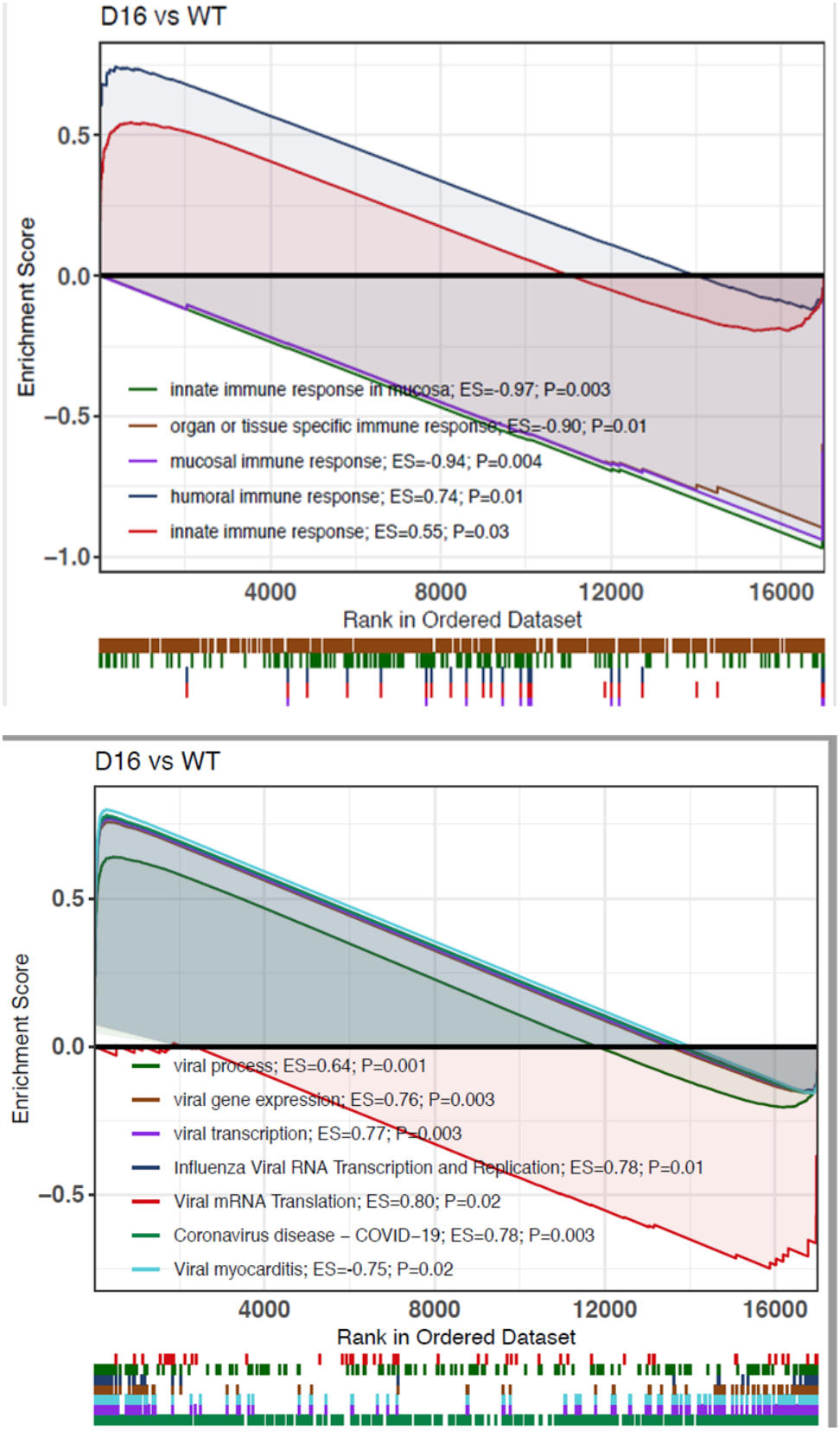

Fig. S2. Gene set enrichment analysis (GSEA) comparing SARS-CoV-2 d16 mutant to WT. Virus infection was performed on A549-ACE2-TMPRSS2 cells, followed by RNA-seq and GSEA analysis. GSEA enrichment plots of two target classes are shown, including mucosal immune response and viral transcription ($P < 0.05$).

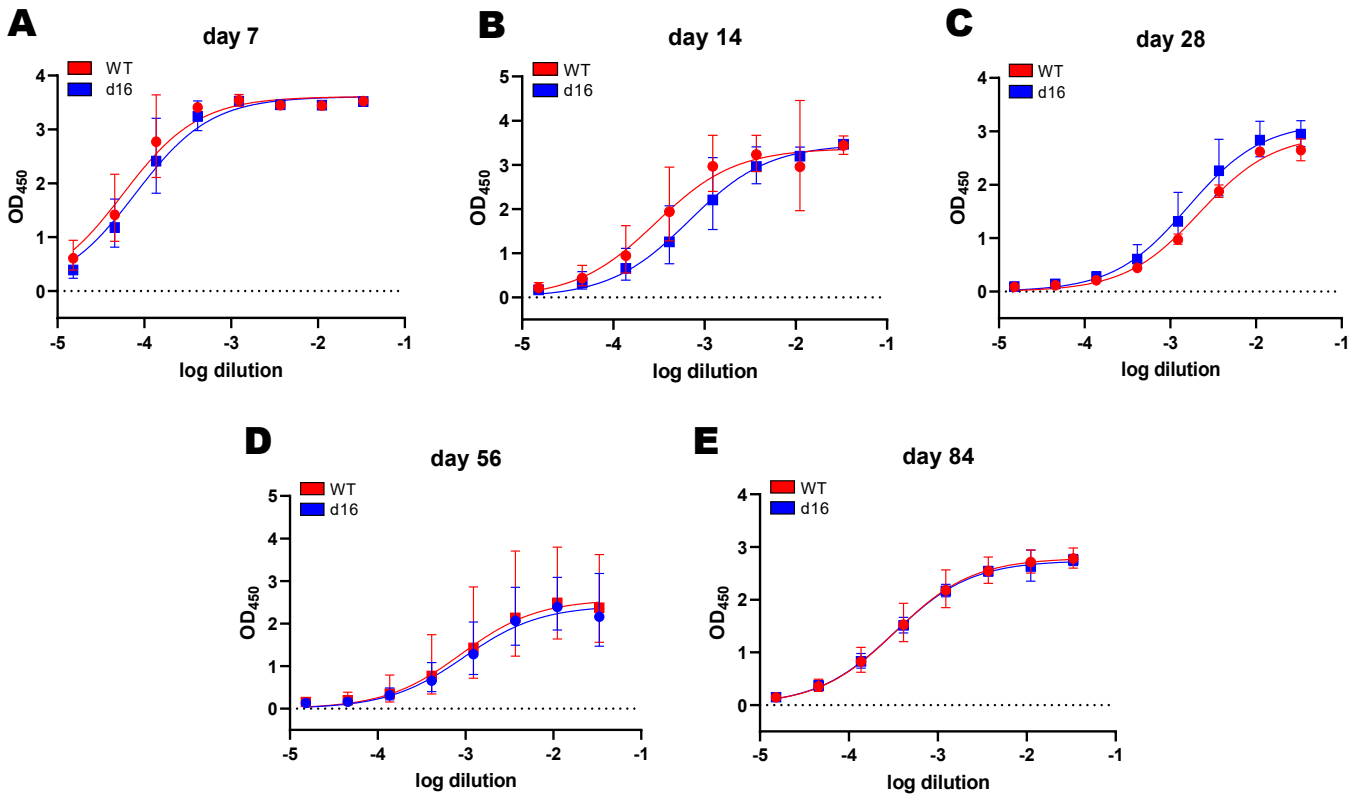

Fig. S3. Antibody response in hamsters infected with SARS-CoV-2 WT and d16 on day 7, 14, 28, 56 and 84, respectively. Serum IgG levels were measured using ELISA for anti-SARS-CoV-2 RBD. Data points presented in geomean ± SEM (n = 5).

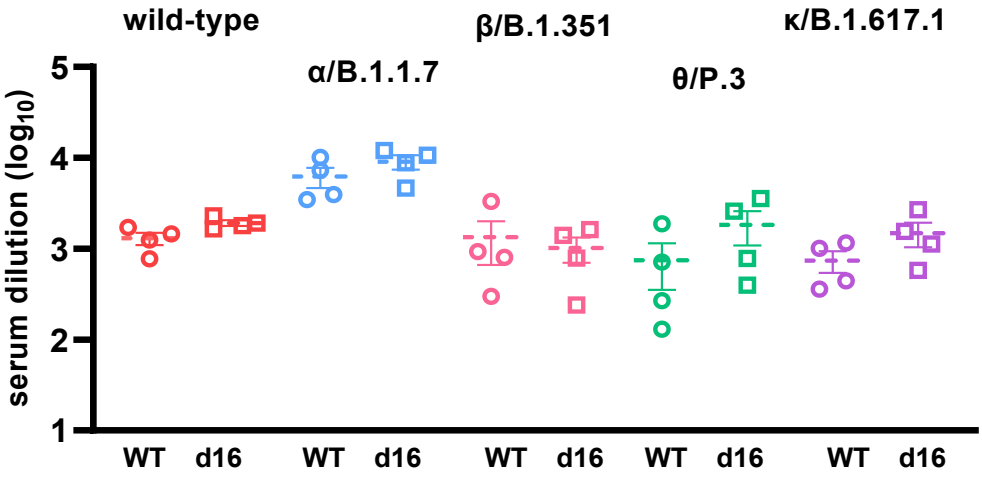

Fig. S4. Antibody response in hamsters infected with SARS-CoV-2 WT and d16 on day 28 against different SARS-CoV-2 variants of concern. Serially diluted hamster sera were tested against WT and various SARS-CoV-2 variants (α, β, θ, and κ) to evaluate their antibodies for neutralizing abilities.

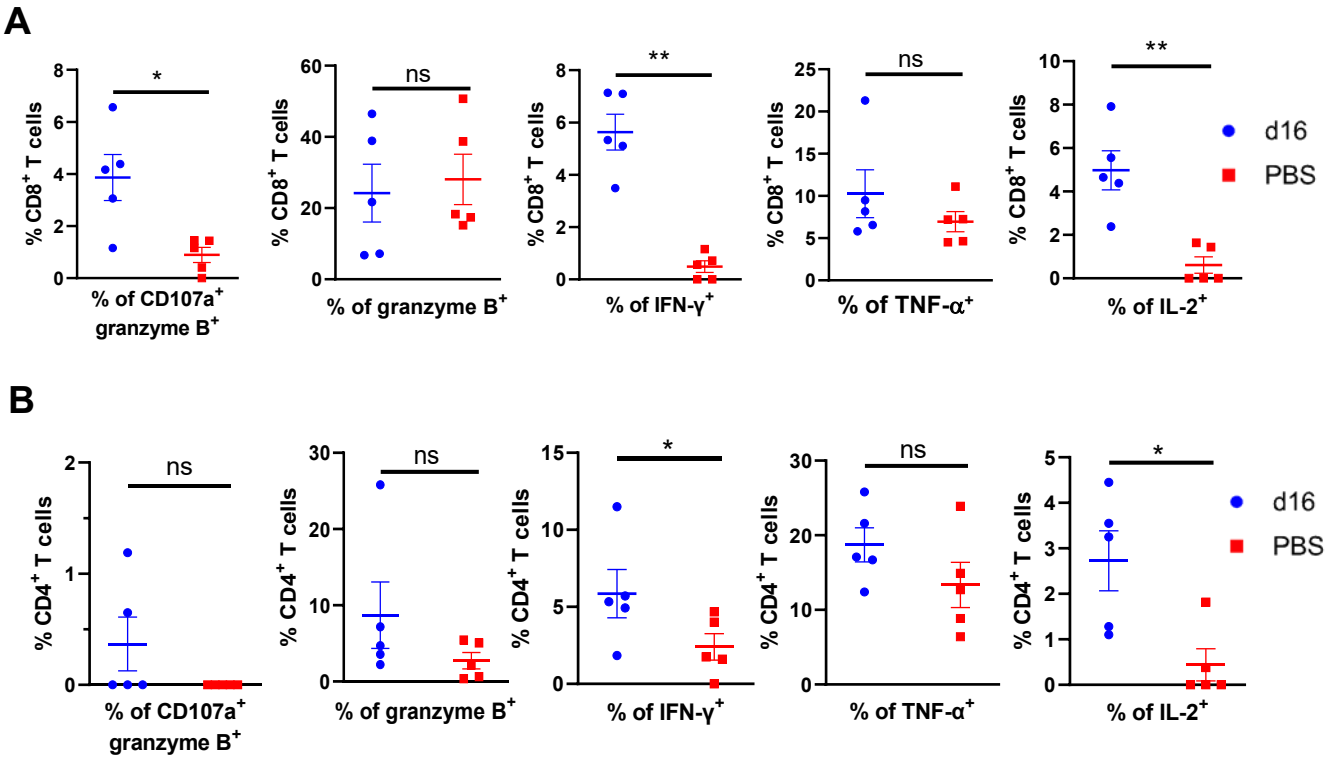

Fig. S5. Related to Fig. 4; T cell immunity elicited by vaccination of K18-hACE2 transgenic mice with d16. K18-hACE2 mice were intranasally vaccinated with 1000 PFU of d16 or PBS (n = 5 mice/group) and challenged with 10000 PFU of clinical isolate HK-13 of SARS-CoV-2 at day 29. Lung-origin T cells were subjected to flow cytometric analysis 4 days post infection. Lung-origin lymphocytes were stimulated with 1 μg/ml of peptide pool of SARS-CoV-2 N protein for 4 h in the presence of brefeldin. Percentages of $CD107a^+$ and cytokine producing $CD8^+$ (A) and $CD4^+$ (B) T cells were also assessed. Results are shown as mean ± SEM. Statistical analyses via Student's t test (*: $P < 0.05$; **: $P < 0.01$; ns: not significant).

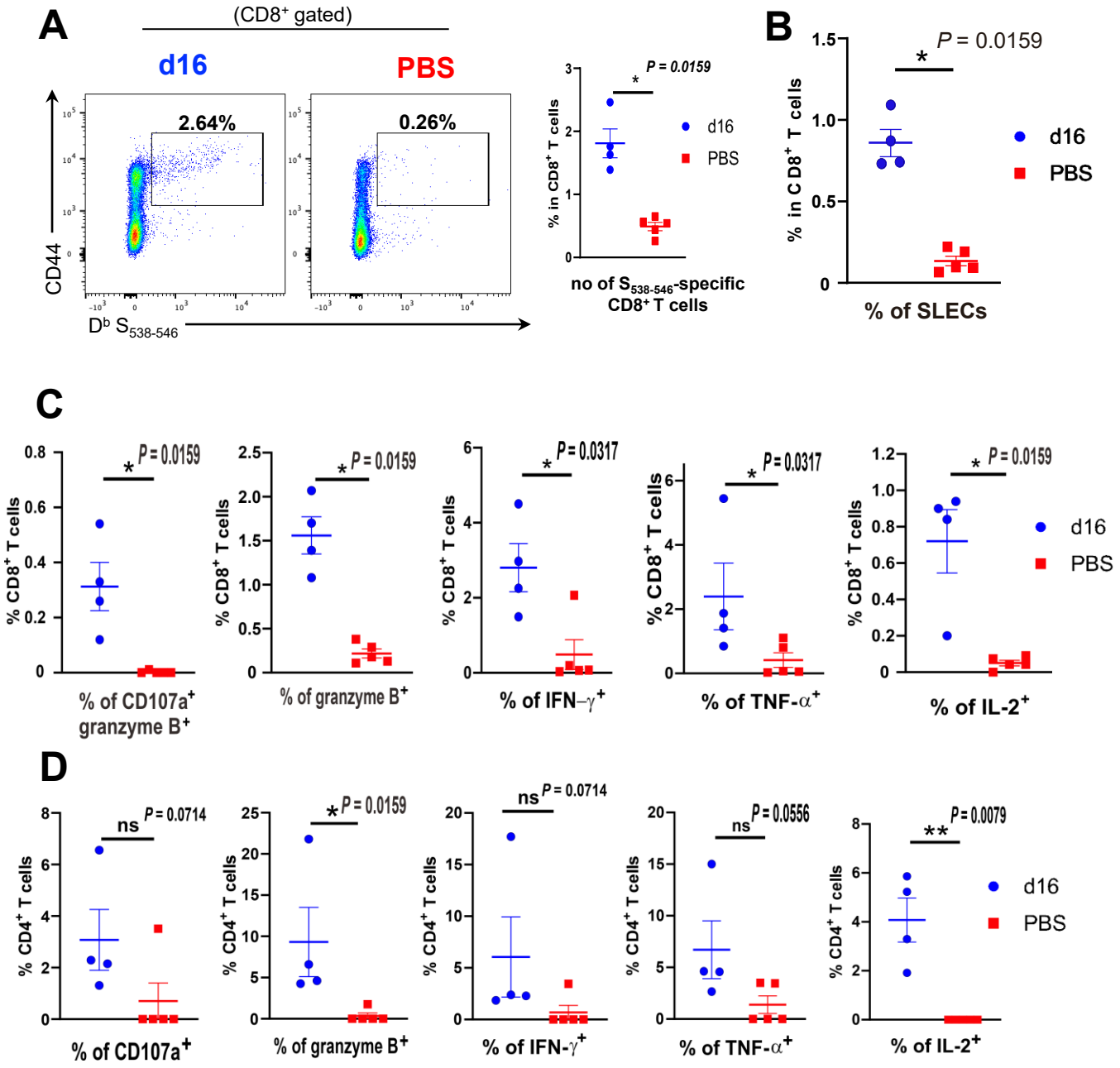

Fig. S6. SARS-CoV-2 d16 elicits robust T cell response in spleen following challenge with HK-13 virus. K18-hACE2 mice were intranasally inoculated with 1000 PFU of SARS-CoV-2 d16 or PBS (n = 4 or 5 mice/group) and challenged with 10000 PFU of SARS-CoV-2 HK-13 strain at day 29 dpi. T cells from spleen were subjected to flow cytometric analysis 4 days later. **A** Representative flow cytometric plots showing percentages of $S_{538-546}$-specific $CD8^+$ T cells. **B** Proportions of short-lived effectors ($KLRG1^+IL\text{-}7R^-$) among total $CD8^+$ T cells. Splenocytes were stimulated with 1 μg/ml of $S_{538-546}$ peptide for 4 h in the presence of brefeldin A. Percentages of cytokine-producing $CD8^+$ (**C**) and $CD4^+$ (**D**) T cells. Results are shown as mean ± SEM. Difference between the indicated groups was statistically significant as judged by Student's t test (*: $P < 0.05$; **: $P < 0.01$; ns: not significant).

A

d16-P10	Amino acid	Nucleotide/amino acid change (compared to d16-P0)
NSP6	119	GCT → GTT / Ala → Val
NSP12	284	ACT → ACC / silent
NSP15	191	GAA → GAC / Glu → Asp
S	95	ACT → ATT / Thr → Ile
	245	CAT → CGT / His → Arg
E	32	GCC → GCT / silent

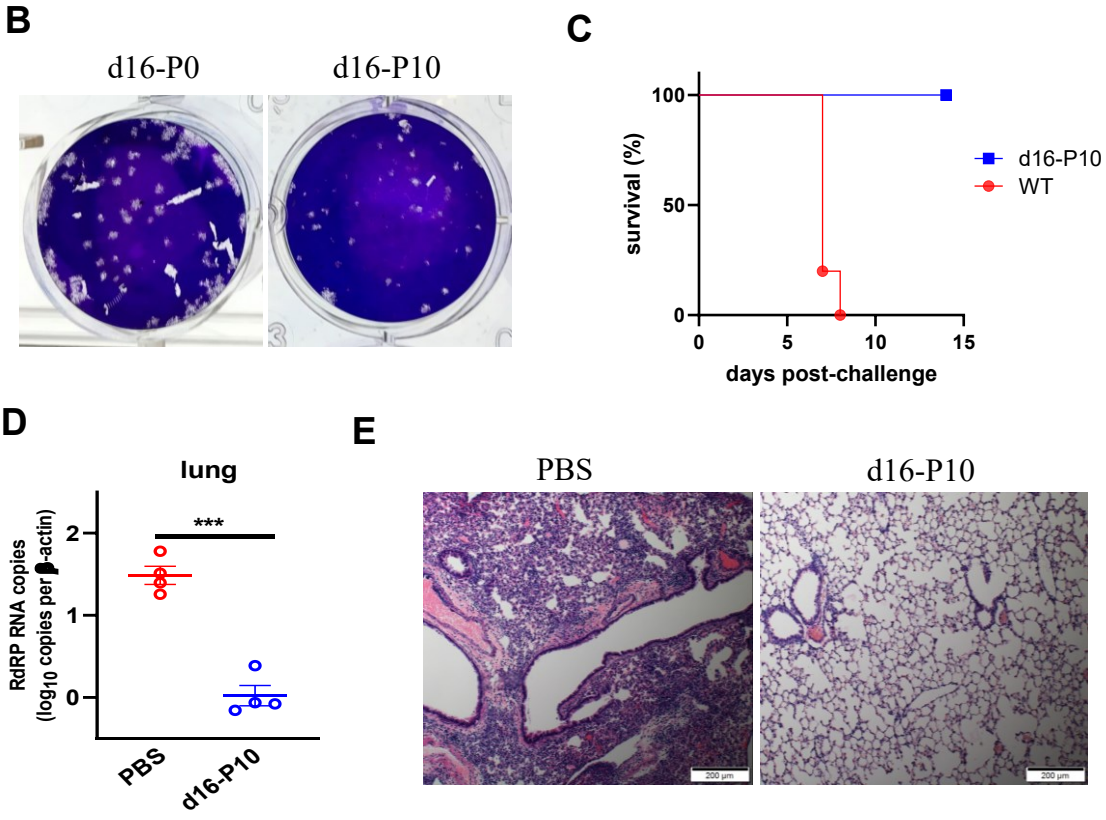

Fig. S7. Further characterization of passage 10 of d16 virus (d16-P10). A A summary of the point mutations found in d16-P10 after passaging in Vero cells by nanopore sequencing [14]. **B** Plaque phenotype. VeroE6-TMPRSS2 cells were infected with the indicated recombinant viruses. After 60 h of incubation at 37°C, cells were fixed and stained with 1% crystal violet. **C** The survival rates of WT- or d16-P10-infected K18-hACE2 transgenic mice (n = 5/group). K18-hACE2 mice were intranasally inoculated with 1000 PFU of recombinant WT or d16-P10 and the survival rate were observed for 14 days. **D** Viral loads by RT-qPCR of lung tissues of SARS-CoV-2-infected mice vaccinated with d16-P10 or PBS at 4 dpi (n = 4/group). Statistical analyses via Student's t test (***: $P < 0.001$). After intranasal vaccination with 1000 PFU of recombinant d16 or PBS, each vaccinated mouse was challenged with 10000 PFU of clinical isolate HK-13 of SARS-CoV-2 at day 29. At day 33, lung tissues were collected for quantification of viral loads using RT-qPCR. **E** Effect of vaccination on the histopathological changes in lungs of SARS-CoV-2-infected vaccinated mice. Representative sections of lung tissue from mice harvested at 4 dpi were stained with H&E.

Table S1. Primers used in this study.

Mutants constructed	Sequences (5′ – 3′)
NSP16 galK forward	TTGGTGATTGTGCAACTGTACATACAGCTAATAAATGG GATCTCATTATT CCTGTTGACAATTAATCATCGGCA
NSP16 galK reverse	CCCTCTTTAGAGTCATTTTCTTTTGTAACATTTTTAGTC TTAGGGTCGTA TCAGCACTGTCCTGCTCCTT
NSP16 D130A forward	TTGGTGATTGTGCAACTGTACATACAGCTAATAAATGG GATCTCATTATTAGTGcTATGTACGACCCTAAGACTAA AAATGTTACAAAAAGAAAATGACTCTAAAGAGGG
NSP16 D130A reverse	CCCTCTTTAGAGTCATTTTCTTTTGTAACATTTTTAGTC TTAGGGTCGTACATA*g*CACTAATAATGAGATCCCATTT ATTAGCTGTATGTACAGTTGCACAATCACCAA

*The galK-complementary sequences are underlined.
**Point mutations are shown in lowercase.

	Sanger sequencing
NSP16 forward	CTACGGGTACGCTGCTTGTC
NSP16 reverse	ATGCGAAGTGTCCCATGAGC
	qPCR
SARS-CoV-2	
RdRp forward	CGCATACAGTCTTRCAGGCT
RdRp reverse	GTGTGATGTTGAWATGACATGGTC
mice	
IL-1β forward	GAAATGCCACCTTTTGACAGTG
IL-1β reverse	TGGATGCTCTCATCAGGACAG
IL-6 forward	CTGCAAGAGACTTCCATCCAG
IL-6 reverse	AGTGGTATAGACAGGTCTGTTGG
IFN-γ forward	CAGCAACAGCAAGGCGAAAAAGG
IFN-γ reverse	TTTCCGCTTCCTGAGGCTGGAT
β-actin forward	AAGGCCAACCGTGAAAAGAT
β-actin reverse	GTGGTACGACCAGAGGCATAC
hamster	
IL-4 forward	ACAGAAAAAGGGACACCATGCA
IL-4 reverse	GAAGCCCTGCAGATGAGGTCT
IL-6 forward	AGACAAAGCCAGAGTCATT
IL-6 reverse	TCGGTATGCTAAGGCACAG
IL-10 forward	GGTTGCCAAACCTTATCAGAAATG
IL-10 reverse	TTCACCTGTTCCACAGCCTTG
TNF-α forward	TGAGCCATCGTGCCAATG
TNF-α reverse	AGCCCGTCTGCTGGTATCAC
CCL17 forward	GTGCTGCCTGGAGATCTTCA
CCL17 reverse	TGGCATCCCTGGGACACT
FOXP3 forward	GGTCTTCGAGGAGCCAGAAGA
FOXP3 reverse	GCCTTGCCCTTCTCATCCA
GAPDH forward	GACATCAAGAAGGTGGTGAAGCA
GAPDH reverse	CATCAAAGGTGGAAGAGTGGGA
β-actin forward	ACTGCCGCATCCTCTTCCT
β-actin reverse	TCGTTGCCAATGGTGATGAC